# Dalton Transactions

Accepted Manuscript






ROYAL SOCIETY OF CHEMISTRY

www.rsc.org/dalton

Journal Name

RSCPublishing

ARTICLE

# Dimethylsilyl Bis(amidinate) Actinide Complexes: Synthesis and Reactivity Towards Oxygen Containing Substrates. †

Cite this: DOI: 10.1039/xoxxoooooox

Received ooth January 2012,
Accepted ooth January 2012

DOI: 10.1039/xoxxoooooox

www.rsc.org/

Isabell S. R. Karmel, Tatyana Elkin, Natalia Fridman, Moris S. Eisen*

The reactivity of the monoanionic amidinate ligand $[(CH_3)_3CNC(Ph)NSiMe_2NC(Ph)\text{-}NHC(CH_3)_3]Li$ (**1**) with a silyl amido side arm towards the early actinides, uranium and thorium, was investigated. While the salt metathesis reaction with $ThCl_4(thf)_3$ afforded the bis(amidinate)thorium(IV) dichloride complex $[(CH_3)_3CNC(Ph)NSi(CH_3)_2NC(Ph)\text{-}NHC(CH_3)_3]ThCl_2$ (**2**) in high yield, the reaction of ligand **1** with $UCl_4$ leads to a Lewis acid supported nucleophilic attack of an incoming ligand unit, yielding the trichloro uranium complex $[(CH_3)_3CNC(Ph)Si(CH_3)_2\text{-}N(C(CH_3)_3)C(Ph)NSi(CH_3)_2NC(Ph)N\text{-}(C(CH_3)_3]UCl_3$ (**4**). The exposure of *in situ* formed complex **2** to wet THF solutions (<1% w of water), gave the mono(amidinate)Th(IV)(chloro)(bis-hydroxo) dimeric complex $[(CH_3)_3CNC(Ph)NSiMe_2\text{-}NC(Ph)NHC(CH_3)_3Th(OH)_2(Cl)]_2\cdot$(**3**) as bright red needles, exhibiting extremely short Th-OH bond distances (1.741(5) Å and 1.737(5) Å). The reactivity of the thorium complex **2** in the ring opening polymerization (ROP) was studied, showing high activity. Thermodynamic and kinetic measurements were performed to shed light on the mechanism for the ROP.

## Introduction

The chemistry of the early actinide elements, thorium and uranium, has undergone a long journey, since the discovery of the first organoactinide complex, $Cp_3UCl$, reported by Wilkinson et al in 1956.[1] Over the past three decades, the organometallic chemistry of these elements has been mainly dominated by cyclopentadienyl derivatives,[2] and has only recently started to be developed towards, heteroatom containing ligand systems.[3,4,5] Amidinate ligands, containing the NCN heteroallylic core, are considered to be steric analogues of the cyclopentadienyl moiety, displaying very similar cone angles of 137° for the cyclopentadienyl, and 136° for the benzamidinate moiety, respectively.[6a,b] Amidinates have found a wide application as ancillary ligands for main group elements, transition metals, lanthanides and actinides.[6c,d] This can be attributed mainly to the availability of the starting materials and ease of synthesis, as well as the easy modification of the steric and electronic properties of the ancillary ligands by variation of the substituents on the nitrogen, and the *ipso*-carbon atoms, allowing for a delicate control of the steric hindrance and electronic properties of the metal complex formed, and therefore allowing a designed manipulation of its reactivity.[7] Despite the steric similarity between cyclopentadienyl and amidinate ligands,[6a,b] their electronic properties are very different. While the cyclopentadienyl moiety is a six electron donor, the amidinate group is only a four electron donor, rendering the respective metal center more electron deficient. The higher electrophilicity of the metal center should in turn increase its oxophilicity and therefore also the reactivity towards oxygen containing molecules, such as water, alcohols, or esters, impeding in most cases their use as catalytic precursors. Amidinate complexes of the lanthanide metals have indeed shown an extraordinary high activity in the ring opening polymerization (ROP) of ε-caprolactone and L-lactide,[8] as well as in the copolymerization of these monomers, yielding biodegradable and biocompatible polymers with a wide range of applications in biomedicine,[9] environmentally friendly packaging materials,[10] microelectronics[11] and adhesives.[12] Despite the fact that the coordination chemistry of the amidinate ligands with the early actinides, uranium and thorium, has been studied previously,[13] only few reports are available regarding the reactivity of these complexes with oxygen containing substrates.[13f,k,l] Recently, we have reported that the activity of coordinative unsaturated uranium (IV) complexes can be modified by adjusting the electronic properties of the ligands. By using highly nucleophilic, strongly basic imidazolin-2-iminato ligands, and therefore increasing the electron density on the highly electrophilic uranium center, the activity in the catalytic ROP of ε-caprolactone reached extremely high values up to $7\cdot10^3$ $kg\cdot mol^{-1}\cdot h^{-1}$.[19g] A conceptual question regards the ability to increase the activity of actinide complexes by tuning the steric hindrance around the metal

center, forming partial coordinative saturated complexes. By using the slightly basic amidinate ligands with a side-arm functionality, the steric hindrance around the metal center is increased, yielding sterically encumbered, coordinatively saturated metal complexes. Moreover, the amidine functionality of the side-arm will increase the electron density on the metal center, by coordination of the nitrogen lone-pair to the actinide center, leading to a reduced electrophilicity and therefore an expected increased catalytic reactivity of the actinide complex towards oxygen containing molecules.

In this study we report the synthesis of the first thorium amidinate complexes $[(CH_3)_3CNC(Ph)NSi(CH_3)_2NC(Ph)NHC(CH_3)_3]ThCl_2$ (**2**) and $[(CH_3)_3CNC(Ph)NSiMe_2NC(Ph)NHC(CH_3)_3Th(OH)_2(Cl)]_2$ (**3**) with a free side arm on the ligand and the catalytic activity of the former in the ROP of ε-caprolactone. Moreover, a comparison between the reactivity of thorium and uranium towards the silicon containing amidinate monoanionic ligand $[(CH_3)_3CNC(Ph)NSiMe_2NC(Ph)NHC(CH_3)_3]Li$ (**1**) is presented. While the synthesis of the thorium complexes **2** and **3** can readily be achieved via a salt metathesis reaction between the lithiated amidinate ligand **1** and $ThCl_4(thf)_3$, the analogue reaction with $UCl_4$ leads to a Lewis acid supported nucleophilic attack of an incoming ligand unit on the dimethylsilyl moiety of the uranium intermediate, leading to the formation of the uranium complex $[(CH_3)_3CNC(Ph)Si(CH_3)_2$-$N(C(CH_3)_3)C(Ph)NSi(CH_3)_2NC(Ph)N(C(CH_3)_3]UCl_3$ (**4**) under the elimination of a lithium amidinate salt. When the neutral amidine $[(CH_3)_3CNHC(Ph)NSiMe_2NC(Ph)NHC(CH_3)_3]$ (**5**) is reacted with $UCl_4$ under the addition of a pyridine, as a mild base, the uranium (IV) complex $[(C(CH_3)_3NHC(Ph)NSi(CH_3)_2NC(Ph)NHC(CH_3)_3]UCl_4$-$(C_5H_5N)$ (**6**) is obtained in moderate yields.

## Results and Discussion

The chemistry of thorium and uranium amidinates systems has been limited to simple benzamidinate and pyridylamidinate complexes.[13] Herein, we report the synthesis and structure of the thorium amidinate complexes **2** and **3**, containing an amidine side arm and its structural effect on the metal center, as well as the reactivity of **2** towards ε-caprolactone. Complex **2** was synthesized by a slow addition of a THF solution of the ligand **1** to a THF solution of $ThCl_4(thf)_3$ at -78°C. Subsequent warming of the solution to room temperature, stirring of the solution for 48 hours and extraction with toluene gave complex **2** in 80 % yield as a slightly yellow powder. Crystallographic measurements were performed on single crystals grown from a concentrated toluene solution, layered with hexane at - 6°C. Since these compounds are very oxophilic, we decided to study their reactivity towards small amounts of water as present in regular THF. Hence, when the same reaction was worked-out in wet THF, containing <1% wt. of water, complex **3** was obtained in 67% yield as red crystals (Scheme 1). Crystallographic data for complexes **2** and **3** are presented in Table 1, selected bond lengths and angles are presented in Tables 2 and 3, respectively. The bis(amidinate) thorium (IV) complex **2** crystallizes in the orthorhombic space group Pccn with one molecule of hexane per unit cell (Figure 1). The thorium center is chelated by two amidinate ligands, two chloro ligands, and additional coordination of the amidine side arms, which completes the coordination number to eight. Both amidinate moieties are equivalent, displaying the same values for bond lengths and angles, leading towards a C2 symmetric complex. The Th-N bond distances display different values for all three coordinated N-atoms, with 2.611(3) Å, 2.374(3) Å and 2.621(3) Å for Th-N1, Th-N3 and Th-N4, respectively, corroborating a non-equal electron distribution in the amidinate core, a highly localized Th-N bond, which is further sustained by the N-C bond distances of the amidinate ligand. While N4-C12 and N1-C1 bond are rather short with values of 1.300(5) Å and 1.303(5) Å respectively, the N3-C12 bond is slightly elongated with a distance of 1.362(5) Å. Häfelinger and Kuske have defined the parameter **ΔCN** = d(C–N) - d(C=N) (where d is the bond length in Å) for the central N–C–N linkage of amidines. This parameter ranges from 0 to 0.178 Å for highly to non-conjugated systems, respectively. In our case, the parameter **ΔCN** values are found to be 0.062 and 0.017 Å for the unsymmetrical coordinated and almost symmetrical non-coordinated ligand, respectively in complex **2.**[14]

Hence, the higher electron density of the N1-C1 and N4-C12 bonds is a result of their weaker electron donation to the thorium center, and therefore weaker Th-N bonds. The higher electron density of the Th-N3 bond can be attributed to the stabilization of the negative charge in the α-position to the dimethyl silyl group (α-carbanion stabilization by silicon). The average Th-N and N-C bond lengths are yet comparable to other thorium (IV) amidinate complexes.[13l] The N3-Th-N1, and N3-Th-N4 angles are comparable with values of 60.41(10)° and 52.24(11)°, respectively. The N1-Th-Cl linkage displays a value of 90.04(8)°, which is slightly larger than the N3-Th-Cl angle of 81.10(8)°. The values of the dihedral angles depend on the spacer group, while the Th-N3-C12-N5 angle shows a value of 32.20°, the Th-N1-Si-N3 angle, with a $SiMe_2$ spacer, displays a value of 15.10°, indicating that the C-atom and Si-atom are not in the same plane. The Th-N1-N3-N4 torsion angle displays a value of 0.80°, showing the formation of a plane by the N1, N3, and N4 atoms with the metal center.

Journal Name RSCPublishing

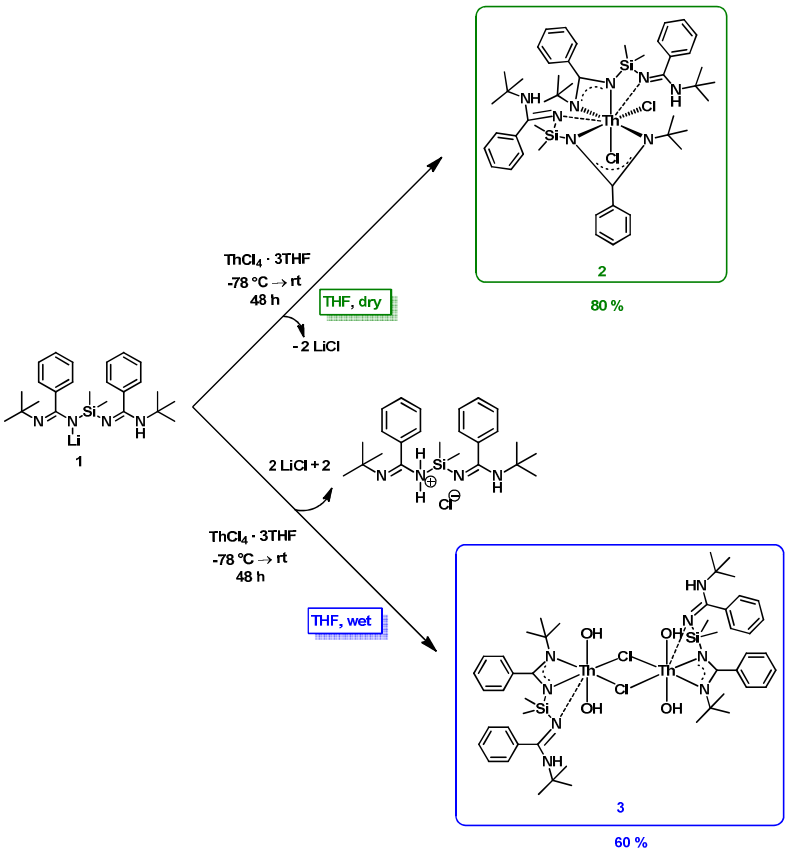


Scheme 1: Synthesis of the thorium amidinate complexes **2** and **3**.

Journal Name RSCPublishing

Table 1 Crystallographic data for complexes **2**, **3**, **4** and **6**.

| **Complex** | **2** | **3** | **4** | **6** |
|---|---|---|---|---|
| Empirical Formula | $C_{52}H_{84}Si_2Cl_2Th$ | $C_{56}H_{82}N_8Si_2Cl_2O_4Th_2$ | $C_{37}H_{55}Cl_3N_6Si_2U$ | $C_{29}H_{41}N_5SiCl_4U$ |
| Formula weight/g·mol$^{-1}$ | 1068.34 | 1522.45 | 984.43 | 867.60 |
| T/K | 250(2) | 250(2) | 240(2) | 250(2) |
| λ/Å | 0.71073 | 0.71073 | 0.71073 | 0.71073 |
| Crystal system | Orthorhombic | Triclinic | Monoclinic | Monoclinic |
| Space group | Pccn | P-1 | P21/C | C 2/C |
| a/Å | 15.7880(5) | 10.9649(6) | 19.5150(4) | 12.2835(4) |
| b/Å | 18.7850(6) | 12.6366(7) | 10.5640(2) | 14.8751(5) |
| c/Å | 20.1863(7) | 12.9693(7) | 22.4540(4) | 23.0777(8) |
| α/° | 90 | 97.368 | 90 | 90 |
| β/° | 90 | 97.368 | 109.1960(9) | 93.3560(10) |
| γ/° | 90 | 98.750 | 90 | 90 |
| V/Å$^3$ | 5986.8(3) | 1696.07(16) | 4371.66(14) | 4209.5(2) |
| Z | 4 | 1 | 4 | 4 |
| ρ/g·cm$^{-3}$ | 1.336 | 1.563 | 1.496 | 1.479 |
| μ(Mo-K$_\alpha$)/mm$^{-1}$ | 2.660 | 4.542 | 3.983 | 4.166 |
| F(000) | 2464 | 786 | 1960 | 1832 |
| Θ range for data collection/° | 1.68 to 25.68 | 1.64 to 25.02 | 1.10 to 25.05 | 1.77 to 26.42 |
| Limiting indices | -19≤ h≤ 19<br>-22≤ k ≤22<br>-24≤ l ≤15 | -13 ≤h≤ 13<br>-15≤ k≤ 15<br>-15≤ l≤ 15 | 0≤ h≤ 23<br>0≤ k≤ 12<br>-26≤ 1≤ 25 | -15≤ h≤ 15<br>-18≤ k≤ 18<br>-28≤ l≤ 28 |
| Reflections collected/unique ($R_{int}$) | 23969/5626 (0.0195) | 62495/5981 (0.0392) | 7747/7747 (0.0000) | 27898/4304 (0.0339) |
| Completeness to Θ | 98.8% | 99.7% | 99.9% | 99.7% |
| GOF on F$^2$ | 1.005 | 1.060 | 1.028 | 1.163 |
| $R_1$, $wR_2$ [I>2σ(I)] | 0.0305, 0.0884 | 0.0354, 0.1074 | 0.0317, 0.0692 | 0.0427, 0.1112 |
| $R_1$, $wR_2$ (all data) | 0.0499, 0.0989 | 0.0384, 0.1092 | 0.0538, 0.0759 | 0.0466, 0.1128 |
| Largest diff. peak and hole (eÅ$^{-3}$) | 1.188 and -0.765 | 3.228 and -0.960 | 0.604, -0.788 | 1.482, -0.895 |

Journal Name RSCPublishing

Table 2: Selected bond lengths and angles for complex **2**.

| Bond lengths (Å) | | Bond Angles (°) | |
|---|---|---|---|
| Th-N1 | 2.611(3) | N3-Th-N1 | 60.41(10) |
| Th-N3 | 2.374(3) | N3-Th-N4 | 52.24(11) |
| Th-N4 | 2.621(3) | N4-Th-N1 | 112.65(9) |
| Th-Cl | 2.6939(11) | N1-Th-Cl | 90.04(8) |
| N1-C1 | 1.303(5) | N3-Th-Cl | 82.99(8) |
| N2-C1 | 1.320(5) | N4-Th-Cl | 81.10(8) |
| N3-C12 | 1.362(5) | Th-N3-C12-N4 | 32.20 |
| N4-C12 | 1.300(5) | Th-N1-Si-N3 | 15.10 |
| | | Th-N1-N3-N4 | 0.80 |
| | | Cl-Th-Cl | 89.9 |

Table 3: Selected bond lengths and angles for complex **3**

| Bond lengths (Å) | | Bond Angles (°) | |
|---|---|---|---|
| Th-O1 | 1.741(5) | O1-Th-O2 | 176.4(2) |
| Th-O2 | 1.737(5) | O1-Th-N1 | 94.5(2) |
| Th-N1 | 2.520(5) | O1-Th-N2 | 93.7(2) |
| Th-N2 | 2.327(5) | O2-Th-N1 | 88.4(2) |
| Th-N3 | 2.623(5) | O2-Th-N2 | 89.7(2) |
| Th-Cl | 2.85536(16) | N1-Th-N2 | 54.22(19) |
| N2-C1 | 1.351(8) | N2-Th-N3 | 60.26(18) |
| N3-C14 | 1.300(9) | O1-Th-Cl1 | 89.94(16) |
| N4-C14 | 1.328(9) | O2-Th-Cl1 | 86.68(15) |
| N1-C1 | 1.304(9) | Th-N2-C1-N1 | 21.70 |
| | | Th-N4-Si-N3 | 19.84 |
| | | Th-N1-N2-N3 | 1.83 |

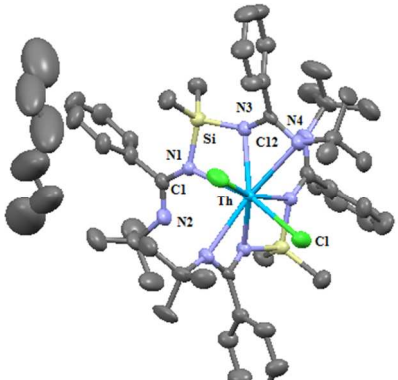


Figure 1: Molecular structure of complex **2**·($C_6H_{14}$) (50% probability ellipsoids). Color code: Th, blue, Cl, green, Si, yellow, N, purple, C, grey. Hydrogen atoms are omitted for clarity.

The dinuclear bridged μ-dichloro thorium (IV) bis(hydroxo) amidinate complex **3** (Figure 2) is obtained in 67% yield when the salt metathesis is carried in dry THF and the work-up of the reaction is performed in wet THF, containing less than 1% wt. water. Complex **3** crystallizes in the triclinic P-1 space group as bright red needles with one molecule of toluene per unit cell. The seven coordinated thorium (IV) center is surrounded by one chelating amidinate ligand, with an amidine side arm coordinated to the metal center, two hydroxo groups, and two μ-chloro ligands bridging between the two thorium centers. The Th-N bond distances display different values for all three Th-N bonds, with 2.520(5) Å, 2.327(5) Å and 2.623(5) Å for Th-N1, Th-N2, and Th-N3, respectively. Similar to complex **2**, the C-N bond distances in complex **3**, also exhibit a slightly uneven electron distribution throughout the amidinate core with values of 1.304(9) Å, 1.351(8) Å, 1.300(9) Å, and 1.328 Å for N1-C1, N2-C1, N3-C14, and N4-C14, respectively. The Häfelinger and Kuske parameter Δ**CN** was calculated to be 0.053 and 0.028 Å for the unsymmetrical coordinated and almost symmetrical non-coordinated ligand, respectively in complex **3.**[14] The higher electron density of the Th-N2 bond can be attributed to the ability of the dimethyl silyl group to stabilize a carbanion in α-position, which is further reflected in the slightly shorter N3-C14 bond distance. The values for the N-Th-N angles depend on the linkage between the nitrogen atoms, while the N1-Th-N2 is 54.22(19), the $SiMe_2$ linkage slightly increases the value of the N2-Th-N3 angle to 60.26(18)°. The dihedral angles display values of 21.70° for Th-N2-C1-N1, and 19.84° Th-N4-Si-N3, indicating different planes for the C-, and Si-atoms. However the N1, N2 and N3 atoms are in the same plane, as shown by the small value of the Th-N1-N2-N3 torsion angle (1.83°). The hydroxo ligands are equivalent, displaying extremely short Th-O distances of 1.741(5) Å and 1.737(5) Å, which are shorter than the average Th-O single bond (Th-O: 1.92 Å – 2.42 Å),[15a,b] and the Th=O double bonds (1.929 Å in a solvated metal complex, and 1.840 Å, in the gas phase[15c,d]). The O1-Th-O2 angle, is close to linearity with a value of 176.4(2)°, and the short Th-O bond length suggest a large electron-donation from the oxygens lone-pairs into the empty orbitals of the metal, leading to a thorium bis(hydroxo) analogue of the uranyl moiety, with similar bond lengths (U=O: 1.725 Å – 2.350 Å, and 1.800 Å in average) and O-M-O angles ($O\text{-}U^{VI}\text{-}O$: 169° - 180°),[16] introducing a new structural motif in the coordination chemistry of actinides. The large electron donation from the oxygen lone pairs, is further reflected in the increasing acidity of the hydroxyl protons, observed in the high downfield shift (10.02 ppm) in $^1$H-NMR spectroscopy. In contrast, the signal of the NH protons (1.42 ppm), displays a slight high field shift as compared to the NH protons (2.21 ppm) in complex **2**. The NH and OH protons can be distinguished by integration of the respective signals in $^1$H-NMR spectroscopy. The increased acidity of the hydroxyl proton in complex **3** is further sustained by the O-H stretching (3340 - 3234 $cm^{-1}$), and the Th-O-H stretch (502 – 416 $cm^{-1}$), which are shifted to lower energies, as compared to previously reported values.[17] The O-Th-N angles are close to 90° with 89.7(2)°, 93.7(2)°, 88.2(2)°, 94.5(2)°, 90.2°, and 90.6(2)° for O2-Th-N2, O1-Th-N2, O2-Th-N1, O1-Th-N1, O2-Th-N3, and O1-Th-N3, respectively. The bridging chlorides display a Th-Cl bond length of 2.8536(16) Å, and a Cl-Th-Cl bond angle of 72.53(5)°. The O-Th-Cl linkages exhibit values close to 90° with 89.94(16)° for O1-Th-Cl1 and 86.68(15)° for O2-Th-Cl1, corroborating a O-Th-O plane,

which is perpendicular to the thorium amidinate and thorium chloride plane.

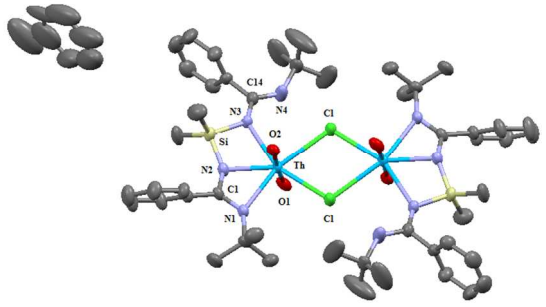


Figure 2: Molecular structure of complex **3·($C_7H_8$)** (50% probability ellipsoids). Color code: Th, blue, Cl, green, Si, yellow, N, purple, O, red, C, grey. Hydrogen atoms are omitted for clarity.

Interestingly, similar to the recently reported μ-chloro thorium (IV) corrole complex,[18] complex **3** crystallizes as unusual bright red crystals. The UV-vis spectrum of complex **3** displays similar absorption bands in the region between 550 nm-300 nm to the reported μ-chloro thorium (IV) corrole compound (see SI). This coloring can probably be attributed to a ligand to metal charge transfer.

The reactivity of ligand **1** towards the uranium (IV) leads to an unexpected nucleophilic attack of an incoming lithiated amidinate moiety on the dimethylsilyl group of the monoamidinate uranium (IV) complex, obtained as an intermediate, after the salt-metathesis with $UCl_4$. The nucleophilic attack is assisted by the coordination to the Lewis acidic uranium (IV) center, and proceeds under the elimination of a lithiated amidine moiety to yield complex **4**[19] (Scheme 3). The absence of free benzonitrile in the reaction mixture indicates that a retro Brook mechanism is not a major operative pathway. The crystallographic data for complex **4** is presented in Table 1, and selected bond length and angles in Table 4, respectively. The uranium complex **4** crystallizes as dark red-brown prisms in the monoclinic P 21/c space group. The geometry around the uranium center can be described as capped trigonal prismatic, with four nitrogen atoms and three chlorides coordinated to the uranium (IV) center (Figure 3). The length of the U-N bond distances varies from 2.533(3) Å for U-N4 to 2.349(4) Å for U-N2, which can be attributed to the nature of bonding of each nitrogen atom in the amidinate ligand.

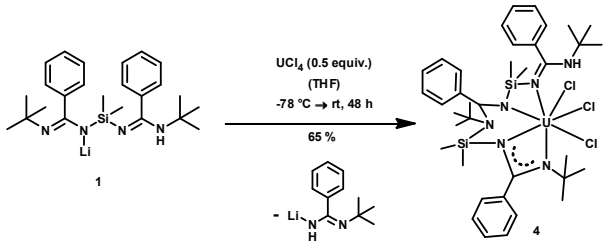


Scheme 2: Synthesis of the uranium complex **4**.

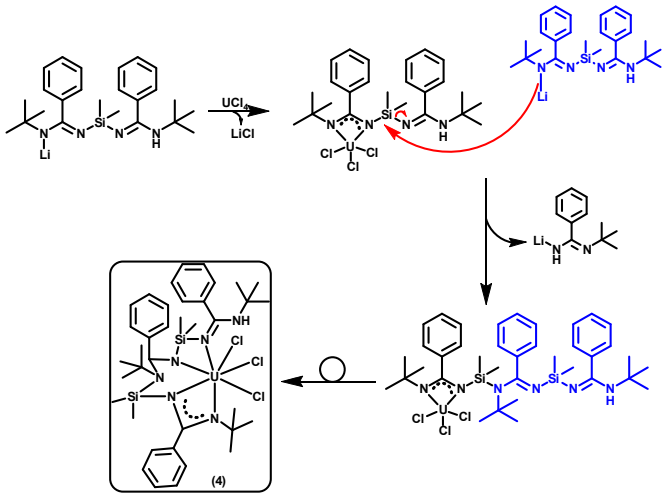


Scheme 3: Plausible mechanism for the synthesis of complex **4**.

Table 4: Selected bond lengths and angles for complex **4**

| Bond lengths(Å) | | Bond angles (°) | |
|---|---|---|---|
| U-N1 | 2.486(4) | N1-U-N2 | 54.95(13) |
| U-N2 | 2.349(4) | N2-U-N4 | 75.53(12) |
| U-N4 | 2.533(3) | N4-U-N5 | 60.96(11) |
| U-N5 | 2.525(4) | N1-U-Cl1 | 115.70(9) |
| U-Cl1 | 2.6233(12) | N1-U-Cl2 | 102.00(9) |
| U-Cl2 | 2.6608(13) | N1-U-Cl3 | 78.86(9) |
| U-Cl3 | 2.6372(12) | N2-U-Cl1 | 94.51(10) |
| N1-C5 | 1.289(5) | N2-U-Cl2 | 156.94(10) |
| N2-C5 | 1.327(5) | N2-U-Cl3 | 84.30(9) |
| Si1-N2 | 1.691(4) | U-N1-C5-N3 | 8.62 |
| Si1-N3 | 1.808(4) | U-N2-N3-N4 | 22.22 |
| Si2-N5 | 1.747(4) | U-N2-Si1-N3 | 58.41 |
| Si2-N4 | 1.762(4) | U-N5-Si2-N4 | 16.59 |

The different lengths of the C-N bonds in the amidine moiety, are 1.289(5) Å and 1.327(5) Å for N1-C5 and N2-C5, respectively. The Häfelinger and Kuske parameter **ΔCN** = 0.037 Å,[14] suggest a slightly uneven electron distribution along the amidine core, which is further reflected in the unequal length of the U-N bonds. This is further sustained by different lengths of the N-Si bonds, with values of 1.691(4) Å for Si1-N2 and 1.808(4) Å for Si1-N3, displaying a shorter N-Si bond closer to the amidine core, which can be accredited to the ability of the dimethyl silyl moiety to stabilize a negative charge in α-position. The U-N4 and U-N5 exhibit similar bond distances with values of 2.533(3) Å and 2.523(4) Å, respectively, which are slightly longer than the distances found for U-N1 and U-N2, indicating an interaction between the a lone pair of the N4 and N5 atoms and the uranium (IV) center. The U-Cl bond distances display similar values of 2.6233(12) Å, 2.6608(13) Å, and 2.6372(12) Å, for U-Cl1, U-Cl2, and U-Cl3, respectively. The N-U-N angles depend on the spacer group, similar to the complexes **2** and **3**. While the N1-U-N2 angles with a C-Ph spacer, shows a value of 54.95(13)°, the N4-U-N5 angles with a $SiMe_2$ spacer group is slightly larger (60.96(11)°). The largest N-U-N angles was found for N2-U-N4 with a value of 75.53(12)°, with a silylamido spacer, forming a six membered ring with the uranium center. The

dihedral angles were determined for U-N1-C5-N3 (8.62°), U-N2-N3-N4 (22.22°), U-N2-Si1-N3 (58.41°), U-N5-Si2-N4 (16.59°). The angle formed between the U-N1-C5-N2 and U-N5-Si2-N4 planes, displays a value of 130°.

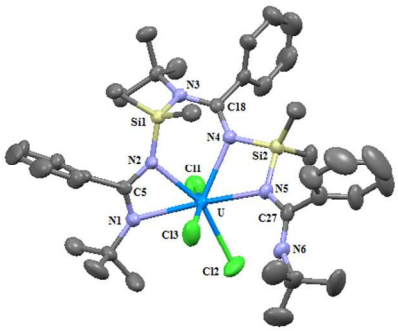


Figure 3: Molecular structure of complex **4** (50% probability ellipsoids). Color code: U, blue, Cl, green, Si, yellow, N, purple, C, grey. Hydrogen atoms are omitted for clarity.

In order to avoid the nucleophilic attack of the lithium amidinate assisted by the uranium complex, we attempted to deprotonate the neutral amidine ligand **5** with pyridine as a mild base, which induced the formation of complex **6** (Scheme 4). Crystallographic data for complex **6** is presented in Table 1, and selected bond lengths and angles in Table 5, respectively.

Table 5: Selected bond lengths and angles for complex **6**.

| Bond lengths (Å) | | Bond angles (°) | |
|---|---|---|---|
| U-N1 | 2.474(5) | N1-U-N1#1 | 62.2(2) |
| U-N3 | 2.727(7) | N1-U-Cl1 | 79.57(11) |
| U-Cl1 | 2.6576(16) | N1-U-Cl2 | 127.43(12) |
| Si-N1 | 2.6277(16) | N3-U-Cl1 | 82.97(4) |
| N1-C1 | 1.315(7) | N3-U-Cl2 | 75.11(5) |
| N2-C1 | 1.333(7) | U-N1-Si-N1 | 0.00 |

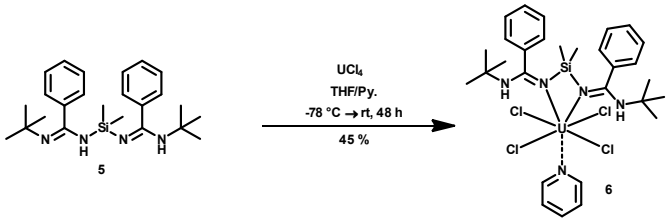


Scheme 4: Synthesis of complex **6** with the neutral amidine **5**.

The uranium (IV) complex **6** crystallizes as green crystals in the monoclinic C2/c space group with one molecule of benzene per unit cell (Figure 4). The U-N1 bond distance is slightly longer than the amidinate U-N1 bond distance in complex **4** with 2.474(5) Å, yet it still lies within the same range of the U-N amidinate bond. The N1-U-N1 linkage is comparable to the N4-U-N5 angle in complex **4** displaying a value of 62.2(2)°. The U-Cl bond distances are similar to those found for complex **4** with values 2.6277(17) Å and 2.6576(16) Å for U-Cl1 and U-Cl2, respectively. The U-N3 bond distance to the coordinated pyridine moiety displays a value of 2.727(7) Å, which is longer than the other U-N distances, as expected.

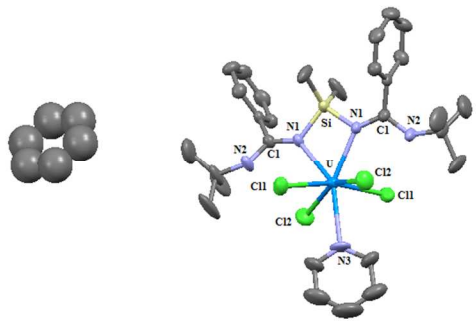


Figure 4: Molecular structure of complex **6·($C_6H_6$)** (50% probability ellipsoids). Color code: U, blue, Cl, green, Si, yellow, N, purple, C, grey. Hydrogen atoms are omitted for clarity.

**Catalytic ring opening polymerization of ε-caprolactone**

The early actinide elements thorium and uranium were long thought to be inactive towards oxygen containing molecules, such as alcohols, aldehydes, esters and cyclic lactones, due to their high electrophilicity and resulting high oxophilicity. Consequently the examples for catalytic conversions of oxygen containing substrates by thorium and uranium are rare, and still remain a challenge in the field of catalysis.[131,20] Herein, we study the reactivity of the thorium complexes **2** and **3** towards the opening of the cyclic ester, ε-caprolactone, leading towards the biodegradable polymer polycaprolactone. The amidinate complexes **2** and **3** containing a pendant side-arm, which donates electron density to the metal-center seem to be good candidates as catalysts for the ROP of ε-caprolactone. While this assumption has been proven to be true for complex **2**, complex **3** doesn't react with ε-caprolactone, which can be attributed to the saturated coordination sphere of **3** in comparison to complex **2**, due to the electron donation of the corresponding hydroxo ligands. The polymerization results for the ROP of ε-caprolactone by complex **2** are presented in Table 6. Since, the uranium (IV) complexes **4** and **6** only display a slight activity towards ε-caprolactone, at elevated temperatures, and no activity at room temperature, these results will not be further discussed.

The polymerization of ε-caprolactone mediated by complex **2** shows an increase in activity and molecular weight of the polymers obtained as a function of time, until all the monomer is consumed after 120 minutes. When the reaction is carried out at elevated temperatures, higher catalytic activities and higher molecular weights of the polymers can be achieved, as expected. The low polydispersity of the polymers together with an increase of the molecular weight as a function of time indicates that the polymerization is performed via a single site catalyst in a quasi-living polymerization fashion. These quasi living situations are expected to be operative due to the different coordination of the growing polymer chain to the metal center. The rates of monomer insertion and chain termination were calculated using equations 1 and 2, respectively.

$$\text{Monomer insertion rate}(Ri) = \frac{m(polymer)[g]}{Mw(monomer)\left[\frac{g}{mole}\right] \times time[h]} \quad (1)$$

$$\text{Chain termination rate}\left(Rt\right)=\frac{m(polymer)[g]}{Mn(polymer)\times time[h]} \quad (2)$$

As the monomer is being consumed, the rates of insertion is reduced, however there is a continuous increase in the molecular weight. In order to obtain the kinetic dependence of the reaction on ε-caprolactone and complex **2**, kinetic NMR measurements were performed, displaying a first-order dependence on the substrate and catalyst **2** (Figure 5) giving raise to the kinetic equation 3.

Table 6: Polymerization results for the ROP of ε-caprolactone mediated by **2**.

| Entry | 2:ε -CL | Time/min | Activity/g·mol$^{-1}$·h$^{-1}$ | $M_w$/Dalton | $M_n$/Dalton | PD | $R_i$/mol·h$^{-1}$ | $R_t$/mol·h$^{-1}$ |
|---|---|---|---|---|---|---|---|---|
| 1 | 1:1000 | 10 | 24900 | 70800 | 48900 | 1.45 | $2.03\cdot10^{-3}$ | $4.75\cdot10^{-6}$ |
| 2 | 1:1000 | 30 | 33680 | 106800 | 82800 | 1.29 | $1.32\cdot10^{-3}$ | $1.81\cdot10^{-6}$ |
| 3 | 1:1000 | 60 | 51590 | 108100 | 69700 | 1.55 | $1.00\cdot10^{-3}$ | $1.25\cdot10^{-6}$ |
| 4 | 1:1000 | 120 | 78210 | 357400 | 266700 | 1.34 | $7.64\cdot10^{-4}$ | $4.31\cdot10^{-7}$ |
| 5 | 1:1000 | 300 | 24480 | 481200 | 422100 | 1.14 | $4.40\cdot10^{-4}$ | $1.18\cdot10^{-7}$ |
| 6[b] | 1:1000 | 120 | 102510 | 634500 | 425800 | 1.49 | $1.00\cdot10^{-3}$ | $2.94\cdot10^{-7}$ |
| 7 | 1:500 | 120 | 22430 | 226600 | 155200 | 1.46 | $5.21\cdot10^{-4}$ | $3.83\cdot10^{-7}$ |
| 8 | 1:2000 | 120 | 230550 | 496900 | 417600 | 1.19 | $2.12\cdot10^{-3}$ | $5.82\cdot10^{-7}$ |

[a] polymerization conditions: 5mL toluene, 2.23 μmol catalyst, rt. [b] 90°C, $R_i$ = Rate of insertion, $R_t$= Rate of termination

$$\frac{\partial \mathrm{p}}{\partial \mathrm{t}} = k_{obs} \cdot [complex\ \mathbf{2}] \cdot [\epsilon - caprolactone] \quad (3)$$

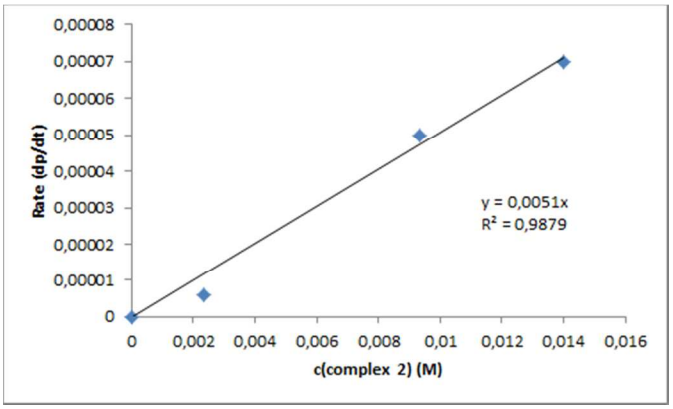


Figure 5: Plot of the rate of polymerization (∂p/∂t) versus concentration of catalyst **2**.

The thermodynamic parameters were determined from the Arrhenius (Figure 6) ($E_a$ = 20.08 kcal/mol) and Eyring ($\Delta H^{\ddagger}$ = 20.02 kcal/mol, $\Delta S^{\ddagger}$ = -12.72 cal/mol·K) plots. A plausible general mechanism for the ROP of ε-caprolactone mediated by the thorium amidinate complex **2** is presented in Scheme 5. At the first step of the mechanism, the substrate ε-caprolactone is rapidly activated by the Lewis acidic thorium complex, to form the Th-alkoxocaprolate complex (**A**).

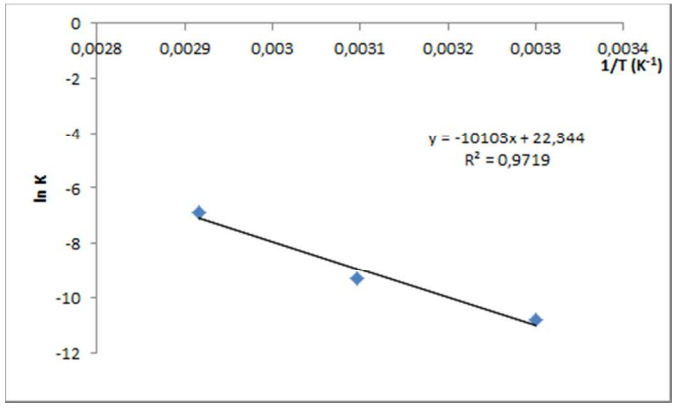


Figure 6: Arrhenius plot for the polymerization of ε-caprolactone mediated by complex **2**.

Insertion of an incoming monomer unit as the rate determining step, leads towards the open chain complex (**B**) that upon additional insertion induces the growing polymer chain (**C**). After hydrolysis with methanol, polycaprolactone with a caprolactonyl end-group can be observed by $^1$H-NMR spectroscopy, supporting the proposed cationic mechanism. $^1$H-NMR experiments with stoichiometric amounts of ε-caprolactone and complex **2**, showed no hydrolysis of the ligand unit upon addition of ε-caprolactone and the formation of complex 2-caprolactone adduct (see SI), reinforcing the coordination of the ligand throughout the polymerization process. Interestingly, the data at hand indicates that the possibility to induce the elimination of the polymer chain with the acidic proton of the ε-caprolactone or the cationic ring is not a major operative pathway, as compared to the insertion of additional monomers (the molecular weight increased as a function of time and the mole number of chains is always lower than the mole of catalyst used) indicating the interaction of the cationic close ring with the metal center.

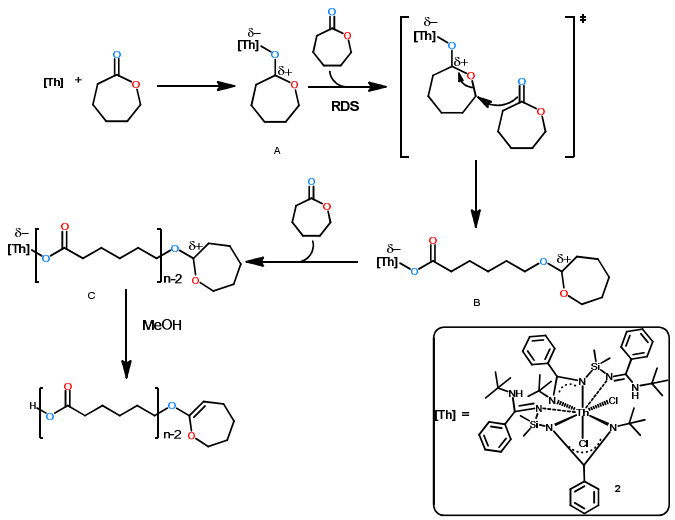


Scheme 5: Plausible mechanism for the ROP of ε-caprolactone mediated by complex **2**.

## Conclusions

The reactivity of the amidinate ligand **1**, containing a silylamidine side chain towards the early actinide elements thorium and uranium was investigated. When **1** was reacted with half an equivalent of $ThCl_4(thf)_3$, complex **2** was obtained in 80% yield. The octahedral amidinate complex **2** displays an additional coordination of the amidine nitrogen to the metal center, completing a coordination number of eight. When the work-up of the salt metathesis reaction of **1** with $ThCl_4(thf)_3$ was carried out in wet THF, complex **3** was obtained as an unusual bright red needle shaped crystals. The thorium centers in complex **3** are bridged by two μ-chloro ligands, leading to a symmetric thorium (IV) dimer. Each of the thorium centers is coordinated by one amidinate moiety, with an additional coordination of the amidine nitrogen, two μ-chloro ligands, and two hydroxo ligands, which are perpendicular to the amidinate-chloro plane. The observed Th-OH bond distances are very short indicating multiple bond order. While complex **2** catalyses the ROP of ε-caprolactone via a cationic "quasi living" mechanism, based on the Lewis acidity of the metal center, complex **3** shows no reactivity towards cyclic lactones and aldehydes. When ligand **1** is reacted with $UCl_4$ complex **4** is obtained by a Lewis acid assisted nucleophilic attack of the same ligand **1** on the dimethylsilyl group of a metal coordinated ligand, as brown-red crystals in a moderate yield. Complex **4** shows only a low reactivity at elevated temperatures towards several oxygen containing substrates, such as ε-caprolactone, and no reactivity towards aromatic aldehydes and alcohols. When the reaction to form complex **4** is worked out in wet THF, the reaction mixture turns instantaneously yellow, suggesting the oxidation to uranium (VI). However, when the reaction of $UCl_4$ with the neutral amidine **5** is carried out under the addition of a mild external base, such as pyridine, complex **6** is isolated, showing a coordination of both amidine nitrogens and an additional pyridine moiety to the $UCl_4$ center. Complex **5** exhibits no activity in the ROP of ε-caprolactone.

## Experimental

All manipulations of air sensitive materials were performed with the rigorous exclusion of oxygen and moisture in flamed Schlenk-type glassware on a high vacuum line ($10^{-5}$torr), or in nitrogen filled MBraun and Vacuum Atmospheres gloveboxes with a medium capacity recirculator (1-2ppm oxygen). Argon and nitrogen were purified by passage through a MnO oxygen removal column and a Davison 4Å molecular sieve column. Analytically pure solvents were dried and stored with Na/K alloy and degassed by 3 freeze-pump-though cycles prior to use (THF, hexane, toluene, benzene-$d_6$, toluene-$d_8$). Amidine **5**,[21] $UCl_4$[22] and $ThCl_4(thf)_3$[23] were synthesized according to published literature procedures. ε-caprolactone and pyridine (Sigma Aldrich) were distilled under reduced pressure from $CaH_2$ and stored in the glovebox prior to use. NMR spectra were recorded on DPX200, Avance 300 and Avance 500 Bruker spectrometers. Chemical shifts for $^1$H-NMR and $^{13}$C-NMR are reported in ppm and referenced using residual proton or carbon signals of the deuterated solvent relative to tetramethylsilane. Elemental analysis was carried out by the microanalysis laboratory at the Hebrew University of Jerusalem. GPC measurements were carried out on a Waters Breeze system with a styrogel RT column and with THF (HPLC grade, T.G. Baker) as mobile phase at 30 °C. Relative calibration was done with polystyrene standards (Aldrich, 2000 – 1800000 range). Mn values were multiplied by a factor of 0.58 and correlated to actual PCL values.

### X-Ray crystallographic measurements

The single-crystal material was immersed in Paratone-N oil and was quickly fished with a glass rod and mounted on a Kappa CCD diffractometer under a cold stream of nitrogen. Data collection was performed using monochromated Mo Kα radiation using φ and ω scans to cover the Ewald sphere.[24] Accurate cell parameters were obtained with the amount of indicated reflections (Table 1).[25] The structure was solved by SHELXS-97 direct methods[26] and refined by the SHELXL-97 program package.[27] The atoms were refined anisotropically. Hydrogen atoms were included using the riding model. Software used for molecular graphics: Mercury 3.1.[28].

### Procedure for the synthesis of $[(CH_3)_3CNC(Ph)NSiMe_2NC(Ph)NHC(CH_3)_3]Li$ (1)

A flame dried Schlenk flask, equipped with a magnetic stirring bar, was charged with $[(CH_3)_3CNHC(Ph)NSiMe_2$-$NC(Ph)NHC(CH_3)_3]$ (**5**) (2.0 g, 4.89 mmol), 50 mL of hexane were added under a constant stream of nitrogen and the colorless solution was cooled to -78°C (acetone/dry ice bath). n-BuLi (3.40 mL, 1.1 equiv., 1.6 M in hexane) was added dropwise via syringe to the $[(CH_3)_3CNHC(Ph)NSiMe_2$-$NC(Ph)NHC(CH_3)_3]$ solution under a constant stream of nitrogen. The yellow reaction mixture was warmed to room

temperature and stirred for 10 hours. Subsequent removal of the solvent and recrystallization from a concentrated hexane solution at -6°C provided the lithium amidinate **1** as a yellow microcrystalline powder (1.90 g, 94%).
$^1$H-NMR ($C_6D_6$, 300.00 MHz) δ -0.27 (s, 6H, Si(C$H_3$)$_2$), 1.21 (s, 9 H, C(C$H_3$)$_3$), 1.14 (s, 9 H, C(C$H_3$)$_3$), 2.45 (brs, 1 H, N$H$), 6.96-7.18 (m, 10 H, $H_{ar}$). $^{13}$C-NMR ($C_6D_6$, 75.00 MHz) δ 3.63 (Si($C$H$_3$)$_2$), 33.54 (C($C$H$_3$)$_3$), 33.76 (C($C$H$_3$)$_3$), 51.31 ($C$(CH$_3$)$_3$), 51.54 ($C$(CH$_3$)$_3$), 132.01 ($C_{ar}$-H), 132.41 ($C_{ar}$-H), 143.54 ($C_{ar}$-C), 175.51 (N$C$(Ph)N). $^{29}$Si-NMR ($C_6D_6$, 60 MHz) δ -16.60 ($Si$(CH$_3$)$_2$). Elemental analysis calculated: C: 69.53, H: 8.51, N: 13.51. Found: 69.98, H: 8.59, N: 13.65.

**Procedure for the synthesis of [(CH$_3$)$_3$CNC(Ph)NSi(CH$_3$)$_2$NC(Ph)NHC(CH$_3$)$_3$]ThCl$_2$ (2)**

A flame dried Schlenk flask, equipped with a magnetic stirring bar and a frit was charged with ThCl$_4$(thf)$_3$ (200 mg, 0.338 mmol) inside the glovebox. A second Schlenk flask was charged with [(CH$_3$)$_3$CNC(Ph)NSiMe$_2$NC(Ph)NHC(CH$_3$)$_3$]Li (**1**) (281 mg, 0.677 mmol) inside the glovebox. THF (ca. 40 mL) was condensed into both flaks using vacuum transfer. The reaction flask, containing ThCl$_4$(thf)$_3$ was cooled to -78°C (acetone/dry ice bath) and the THF solution of the amidinate ligand was added slowly via a syringe to the ThCl$_4$(thf)$_3$ solution under a constant stream of argon. Then, the reaction mixture was warmed slowly to room temperature and stirred for 48 hours. The solvent was removed, the solid residue washed with hexane (3 X 15 mL) and the product **2** was isolated as a slightly yellow powder (303 mg, 80%). Crystals suitable for X-ray crystallography were obtained from a hexane layered toluene solution at -6°C.
$^1$H-NMR ($C_6D_6$, 300.00 MHz) δ 0.02 (s, 6 H, Si(C$H_3$)$_2$), 1.49 (s, 9H, C(C$H_3$)$_{3\ bound}$), 1.65 (s, 9H, C(C$H_3$)$_{3\ side\text{-}arm}$), 2.12 (br, 1H, N$H$), 7.08-7.17 (m, 5H, H$_{ar}$), 7.51-7.53 (m, 5H, H$_{ar}$). $^{13}$C-NMR ($C_6D_6$, 75.00 MHz) δ 3.5 (Si($C$H$_3$)$_2$, 34.0 (C($C$H$_3$)$_{3\ bound}$), 34.6 (C($C$H$_3$)$_{3\ side\text{-}arm}$), 53.4 ($C$(CH$_3$)$_{3\ bound}$), 54.6 ($C$(CH$_3$)$_{3\ side\text{-}arm}$), 128.0-131.0 ($C_{ar}$-H), 135.1 ($C_{ar}$-C) 145.1 (N$C$N), 171.6 (N$C$NH). $^{29}$Si-NMR ($C_6D_6$, 60 MHz) δ -22.89 ($Si$(C(CH$_3$)$_2$). Elemental analysis calculated: C: 41.53, H: 5.69, N: 6.46, Cl: 16.34; Found: C: 41.97, H: 5.71, N: 6.39, Cl: 16.41.

**Procedure for the synthesis of [(CH$_3$)$_3$CNC(Ph)NSiMe$_2$NC(Ph)NHC(CH$_3$)$_3$Th(OH)$_2$(Cl)]$_2$·C$_7$H$_8$ (3)**

A flame dried Schlenk flask, equipped with a magnetic stirring bar and a frit was charged with ThCl$_4$(thf)$_3$ (200 mg, 0.338 mmol) inside the glovebox. A second Schlenk flask was charged with [(CH$_3$)$_3$CNC(Ph)NSiMe$_2$NC(Ph)NHC(CH$_3$)$_3$]Li (**1**) (281 mg, 0.677 mmol) inside the glovebox. THF (ca. 40 mL) was condensed into the flask with the ligand using vacuum transfer and THF (ca. 40 mL) was added to the flask containing ThCl$_4$(thf)$_3$. The reaction flask, containing ThCl$_4$(thf)$_3$ was cooled to -78°C (acetone/dry ice bath) and the THF solution of the amidinate ligand was added slowly via a syringe to the ThCl$_4$(thf)$_3$ solution under a constant stream of argon. The reaction mixture was warmed slowly to room temperature, distilled water (0.50 mL) was added via a syringe under a constant stream of argon to the colourless solution, which instantaneously turned bright red upon the addition of water and the solution was stirred for 48 hours at room temperature. The solvent was removed, the solid residue washed with hexane (3 X 15 mL) and the product (**3**) was isolated as dark red powder (345 mg, 67%). Crystals suitable for X-ray crystallography were obtained from toluene solution at -6°C.
$^1$H-NMR (THF-d$_8$, 300.00 MHz) δ 1.25 (s, 18 H, C(C$H_3$)$_{side\text{-}arm}$), 1.42 (br, 2 H, N$H$), 1.50 (s, 18 H, C(C$H_3$)$_{bound}$), 2.30 (s, 12 H. Si(C$H_3$)$_2$), 7.00-7.46 (m, 20 H, Har), 10.02 (br, 4 H, O$H$). $^{13}$C-NMR (THF-d$_8$, 125.00 MHz) δ = 3.6 (Si($C$H$_3$)$_2$), 32.1 (C($C$H$_3$)$_{3\ side\text{-}arm}$), 34.5 (C($C$H$_3$)$_{3\ bound}$), 54.3 ($C$(CH$_3$)$_{3\ side\text{-}arm}$), 55.9 ($C$(CH$_3$)$_{3\ bound}$), 126.2-130.6 ($C_{ar}$-H), 139.2 ($C_{ar}$-C), 145.2 ($C_{ar}$-C), 169.0 (N$C$NH), 172.0 (N$C$N). $^{29}$Si-NMR (THF-d$_8$) δ -19.0 ($Si$(CH$_3$)$_2$). Elemental analysis calculated: C: 44.74, H: 5.46, N: 7.59, Cl: 4.80. Found: C: 44.68, H: 5.55, N: 7.58, Cl: 4.45.

**Procedure for the synthesis of [(CH$_3$)$_3$CNC(Ph)Si(CH$_3$)$_2$-N(C(CH$_3$)$_3$)C(Ph)NSi(CH$_3$)$_2$NC(Ph)N(C(CH$_3$)$_3$]UCl$_3$·C$_7$H$_8$ (4)**

A flame dried Schlenk flask, equipped with a magnetic stirring bar and a frit was charged with UCl$_4$ (200 mg, 0.527 mmol) inside the glovebox. A second Schlenk flask was charged with [(CH$_3$)$_3$CNC(Ph)NSiMe$_2$NC(Ph)NHC(CH$_3$)$_3$]Li (**1**) (437 mg, 1.054 mmol) inside the glovebox and THF (ca. 40 mL) was condensed into both flaks using vacuum transfer. The reaction flask, containing UCl$_4$ was cooled to -78°C (acetone/dry ice bath) and the THF solution of the amidinate ligand was added slowly via a syringe to the UCl$_4$ suspension under a constant stream of argon. The reaction mixture was warmed slowly to room temperature and stirred for 48 hours. The solvent was removed and the solid residue washed with hexane (3 X 15 mL) and the product (**4**) was isolated as a brown powder (338 mg, 65%). Crystals suitable for X-ray crystallography were obtained from a concentrated toluene solution at -6°C.
$^1$H-NMR ($C_6D_6$, 300.00 MHz) δ -24.14 (s, 6 H, Si(C$H_3$)$_3$, FWHM 2.93 Hz), -17.62 (s, 3 H, Si(C$H_3$)$_3$, FWHM 3.59 Hz), -17.00 (s, Si(C$H_3$)$_3$, FWHM 3.08 Hz), 0.30 (s, 9H, C(C$H_3$)$_{3\ bound}$, FWHM 2.59 Hz), 1.36 (s, 9 H, NC(C$H_3$)$_3$, FWHM 9.03 Hz), 1.65 (s, 9 H, C(C$H_3$)$_{3\ side\text{-}arm}$, FWHM 9.12 Hz), 5.57 (m, 5 H, $H_{ar}$, FWHM 2.77 Hz), 6.49 (m, 5 H, $H_{ar}$, FWHM 3.78 Hz), 7.28 (m, 5 H, $H_{ar}$, FWHM 5.06 Hz), 14.73 (brs, 1 H, N$H$, FWHM 4.63 Hz). $^{13}$C-NMR ($C_6D_6$, 125.00 MHz) δ 0.9 (Si($C$H$_3$), 29.9 (C($C$H$_3$)$_{3\ bound}$), 31.2 (NC($C$H$_3$)$_3$), 38.1 (C($C$H$_3$)$_{3\ side\text{-}arm}$) 52.9 ($C$(CH$_3$)$_{3\ bound}$), 53.3 (N$C$(CH$_3$)$_3$), 62.9 ($C$(CH$_3$)$_{3\ side\text{-}arm}$), 121.5-133.7 ($C_{ar}$-H), 141.5-144.4 ($C_{ar}$-C), 185.5 (N$C$N), 184.2 (NH$C$N), 197.1 (N$C$NH). $^{29}$Si-NMR ($C_6D_6$, 60.00 MHz) δ -21.5 ($Si$(CH$_3$)$_2$). Elemental analysis calculated: C: 45.14, H: 5.63, N: 8.54, Cl: 10.80. Found: C: 45.55, H: 5.71, N: 8.46, Cl: 10.76.

**Procedure for the synthesis of $[(C(CH_3)_3NHC(Ph)NSi(CH_3)_2N-C(Ph)NHC(CH_3)_3]UCl_4(C_5H_5N)\cdot C_6H_6$ (6)**

A flame dried Schlenk flask, equipped with a magnetic stirring bar and a frit was charged with $UCl_4$ (200 mg, 0.527 mmol) inside the glovebox. A second Schlenk flask was charged with $[(CH_3)_3CNC(Ph)NHSiMe_2NC(Ph)NHC(CH_3)_3]$ (**5**) (437 mg, 1.054 mmol) inside the glovebox and THF (ca. 40 mL) was condensed into both flaks via vacuum transfer. The reaction flask, containing $UCl_4$ was cooled to -78°C (acetone/dry ice bath) and the THF solution of the amidinate ligand was added slowly via syringe to the $UCl_4$ suspension under a constant stream of argon. The reaction mixture was warmed slowly to room temperature and pyridine (5 mL) was added via syringe under a constant stream of argon. The brown reaction mixture was stirred for 48 hours at room temperature. The solvent was removed and the solid residue washed with hexane (3 15 mL) and the product (**5**) was isolated as a brown powder (206 mg, 45%). Crystals suitable for X-ray crystallography were obtained from a concentrated benzene solution at 6°C.
$^1$H-NMR (THF-$d_8$, 200.00 MHz) δ 0.87 (s, 6 H, $Si(CH_3)_2$, FWHM 20.97), 1.14 (s, 18 H, $C(CH_3)_3$, FWHM 5.69), 2.26 (br, 2 H, NH, FWHM 6.54), 6.93-7.40 (m, 10 H, $H_{ar}$, FWHM 2.13). $^{13}$C-NMR (THF-$d_8$, 50.00 MHz) δ 3.0 ($Si(CH_3)_2$), 32.7 ($C(CH_3)_3$), 51.5 ($C(CH_3)_3$), 131.1-132.4 ($C_{ar}$-H), 143.5 ($C_{ar}$-C), 175.5 (NHCN). $^{29}$Si-NMR (THF-$d_8$, 60 MHz) -18.7 ($Si(CH_3)_2$). Elemental analysis calculated: C: 44.45, H: 5.01, N: 7.41, Cl: 15.00. Found: C: 44.96, H: 5.01, N: 7.45, Cl: 15.04.

**General procedure for the catalytic polymerization of ε-caprolactone mediated by complex 2**

A sealable J-Young glass tube, equipped with a magnetic stirring bar, was loaded with 2.5 mg of complex **2** from a stock solution, the required amount of ε-caprolactone and 5 mL of dry toluene inside the glovebox. The polymerization was carried out under strong stirring for the required amount of time and temperature. Then, the reaction was quenched by the addition of methanol. After removing the solvent under reduced pressure, the polymer was precipitated from cold methanol, isolated by filtration, washed with three portions of cold methanol (3 X 20 mL) and dried overnight under vacuum. The activity was determined as PCL (g) / mol(cat)·time(h). A sample of the obtained PCL (40 mg) was dissolved in THF and used for determination of the molecular weight.
For the kinetic $^1$H-NMR studies a J-Young NMR tube was loaded with the respective amount of complex **2** from a stock solution, ε-caprolactone and toluene-$d_8$ were added inside the glove box and the tube was sealed. The reaction mixture was frozen at liquid nitrogen temperatures, until staring the $^1$H-NMR measurements. The sample was heated (if required) inside the NMR spectrometer. Similar experiments were performed for the thermodynamic studies.

## Acknowledgements

This research was supported by the USA-Israel Binational Science Foundation under Contract 2010109.

Notes and references

† Schulich Faculty of Chemistry, Institute of Catalysis Science and Technology, Technion – Israel Institute of Technology, Technion City, 32000 Israel.

Electronic Supplementary Information (ESI) available: [details of any supplementary information available should be included here]. See DOI: 10.1039/b000000x/

## References

1. L. T. Reynolds, G. Wilkinson, *J. Inorg. Nucl. Chem*., 1956, **2**, 246.
2. (a) M. Sharma, M. S. Eisen, Struct. Bond. 2008, 427, 1. (b) T. Andrea, M. S. Eisen, Chem Soc. Rev., 2008, 37, 550. (c) R. J. Batrice, I.-S. R. Karmel, M. S. Eisen, Product Class 13: Organometallic Complexes of the Actinides. In: Science of Synthesis Knowledge Updates 2012/4; A. Fuerstner, D. Hall, I. Marek, M. Oestreich, E. Schaumann, B. M. Stoltz, Eds.; Georg Thieme Verlag KG, Stuttgart Germany, 2013, pp. 99-211 and reference cited therein.
3. (a) D. E. Smiles, G. Wu, T. W. Hayton, *J. Am. Chem. Soc.*, 2014, **136**, 96. (b) W. W. Lukens, N. M. Edelstein, N. Magnani, T. W. Hayton, S. Fortier, L. A. Seaman, *J. Am. Chem. Soc.,* 2013, **135**, 10742. (c) J. L. Brown, G. Wu, T. W. Hayton, *Organometallics*, 2013, **32**, 1193. (d) J. L. Brown, S. Fortier, R. A. Lewis, G. Wu, T. W. Hayton, *J. Am. Chem. Soc*., 2012, *134*, 15468. (e) D. D. Schnaars, A. J. Gaunt, T. W. Hayton, M. B. Jones, I. Kirchner, N. Kaltsoyannis, I. May, S. D. Reilly, B. L. Scott, G. Wu, *Inorg. Chem.*, 2012, **51**, 8857. (f) S. M. Franke, F. W. Heinemann, K. Meyer, *Chem. Sci.*, 2014, **5**, 942. (g) B. L. Tran, J. Krzystek, A. Ozarowski, C.-H. Chen, M. Pink, J. A. Karty, J. Telser, K. Meyer, D. L. Mindiola, *Eur. J. Inorg. Chem.*, 2013, 3916. (h) H. La Pierre, S. Henry, K. Meyer, *Inorg. Chem.*, 2013, **52**, 529. (i) O. P. Lam, S. M. Franke, F. W. Heinemann, K. Meyer, *J. Am. Chem. Soc.*, 2012, **134**, 15468. (j) O. P. Lam, L. Castro, B. Kosog, F. W. Heinemann, L. Maron, K. Meyer, *Inorg. Chem.*, 2012, **51**, 781. (k) M. J. Monreal, R. J. Wright, D. E. Morris, B. L. Scott, J. T. Golden, P. P. Power, J.L. Kiplinger, *Organometallics*, 2013, **32**, 1423. (l) E. J. Schelter, R. Wu, J. M. Veauthier, E. D. Bauer, C. H. Booth, R. K. Thomson, C. R. Graves, D. K. John, B. L. Scott, J. D. Thompson, D. E. Morris, J. L. Kiplinger, *Inorg. Chem*., 2010, **49,** 1995.
4. (a) E. M. Matson, W. P. Forrest, P. E. Fanwick, S. C. Bart, *Organometallics*, 2013, **32**, 1484. (b) E. M. Matson, P. E. Fanwick, S. C. Bart, *Eur. J. Inorg. Chem.*, 2012, 5471. (c) E. M. Matson, M. G. Crestani, P. E. Fanwick, S. C. Bart, *Dalton Trans.*, 2012, **41**, 7952. (d) S. J. Kraft, P. E. Fanwick, S. C. Bart, *J. Am. Chem. Soc.*, 2012, **134**, 6160. (e) E. M. Matson, P. E. Fanwick, S. C. Bart, *Organometallics*, 2011, **30**, 5753. (f) V. Mougel, L. Chatelain, J. Hermle, R. Caciuffo, E. Colineau, F. Tuna, N. Magnani, A. de Geyer, J. Pécaut, M. Mazzanti, *Angew. Chem. Int. Ed. Engl*., 2014, **53**, 5′819. (g) C. Clement, M. A. Antunes, G. Garcia, I. Ciofini, I. C. Santos, J. Pécaut, M. Almeida, J. Marcalo, M. Mazzanti, *Chem. Sci*., 2014, **5**, 841. (h) E. Mora, L. Maria, B. Biswas, C. Camp, I. C. Santos, J. Pécaut, A. Cruz, J. M. Carretas, J. Marcalo, M. Mazzanti, *Organometallics*, 2013, **32**, 1409. (i) C. Clement, J. Andrez, J. Pécaut, M. Mazzanti, *Inorg. Chem.*, 2013, **52**, 7078. (j) C. Clement, J. Pécaut, M. Mazzanti, *J. Am. Chem. Soc*., 2013, **135**, 12101. (k) V. Mougel, J. Pécaut, M. Mazzanti, *Chem. Commun.*, 2012, **48**, 868.
5. (a) A. J. Wooles, W. Lewis, A. J. Blake, S. T. Liddle, Organometallics, 2013, 32, 5058. (b) P. Dipti, J. McMaster, W. Lewis, A. J. Blake, S. T. Liddle, Nat. Commun. 2013, 4, 2323. (c) D. M. King, F. Tuna, E. J. L. McInnes, J. McMaster, W. Lewis, A. J. Blake, S. T. Liddle, Nat. Chem., 2013, 5, 482. (d) P. Dipti, F. Tuna, E. J. L. McInnes, J. McMaster, W. Lewis, A. J. Blake, S. T. Liddle, Dalton Trans. 2013, 42, 5224. (e) O. J.

Cooper, D. P. Mills, J. McMaster, F. Tuna, E. J. L. McInnes, W. Lewis, A. J. Blake, S. T. Liddle, Chem. Eur. J., 2013, 19, 7071. (f) D. M. King, F. Tuna, E. J. L. McInnes, J. McMaster, W. Lewis, A. J. Blake, S. T. Liddle, Science, 2012, 337, 717. (g) D. P. Mills, O. J. Cooper, F. Tuna, E. J. L. McInnes, E. S. Davies, J. McMaster, F. Moro, W. Lewis, A, J. Blake, S. T. Liddle, J. Am. Chem. Soc., 2012, 134, 10047. (h) A. R. Fox, S. Creutz, C. C. Cummins, Dalton Trans., 2010, 39, 6632. (i) C.L. Webster, J. W. Ziller, W. J. Evans, Organometallics, 2012, 31, 7191. (j) P. L. Arnold, J. H. Farnaby, R. C. White, N. Kaltsoyannis, M. G. Gardiner, J. B. Love, Chem. Sci., 2014, 5, 756. (k) S. M. Mansell, J. H. Farnaby, A. I. Germeroth, P. L. Arnold, Organometallics, 2013, 32, 4214. (l) G. M. Jones, P. L. Arnold, J. B. Love, Chem. Eur. J., 2013, 19, 10287. (m) P. L. Arnold, S. M. Mansell, L. Maron, D. McKay, Nature Chem., 2012, 4, 668. (n) P. L. Arnold, G. M. Jones, S. O. Odoh, G. Schreckenbach, N. Magnani, J. B. Love, Nature Chem., 2012, 4, 221. (o) J. M. Guy, P. L. Arnold, J. B. Love, Angew. Chem. Int. Ed. Engl., 2012, 51, 12584.

6. (a) A. Recknagel, F. Knösel, H. Gornitzka, M. Noltemeyer, F. T. Edelmann, *J. Organomet. Chem*., 1991, **417**, 363. (b) F. T. Edelmann, *Struct. Bond*., 2010, **137**, 109. (c) J. Barker, M. Kilner, *Coord. Chem. Rev*., 1994, 219. (d) F. T. Edelmann, Advances in the Coordination Chemistry of Amidinate and Guanidinate Ligands, In: *Advances in Organometallic Chemistry, Volume 57*, A. F. Hill, M. J. Fink, Eds., Elsevier: The Netherlands, 2008, pp. 183-252. And references cited therein.
7. (a) S. Aharonovich, M. Botoshanski, B. Tumanskii, K. Nomura, R. M. Waymouth, M. S. Eisen, *Dalton Trans*., 2010, **39**, 5643. (b) S. Aharonovich, M. Botoshanski, Z. Rabinovich, R. M. Waymouth, M. S. Eisen, *Inorg. Chem*., 2010, **49**, 1220. (c) J.-F. Sun, S.-J. Chen. Y, Duan, Y.-Z. Li, X. T. Li, X.-T. Chen, Z.-L. Xue, *Organometallics*, 2009, **28**, 3008. (d) T. Elkin, S. Aharonovich, M. Botoshansky, M. S. Eisen, *Organometallics*, **31**, 7404. (e) T. Elkin, N. V. Kulkarni, B. Tumanskii, M. Botoshansky, L. W. Shimon, M. S. Eisen, *Organometallics*, 2013, **32**, 6337. (f) T. Elkin, S. Aharonovich, M. Botoshansky, M. S. Eisen, *Organometallics*, **31**, 7404.
8. (a) N. Nomura, A. Taira, T. Tomioka, M. Okada, *Macromolecules*, 2000, **33,** 1497-1499. (b) I. Palard, A. Soum, S. M. Guillaume, *Chem. Eur. J.*, 2004, **10**, 4054-4062. (c) Y. Fugen, L. Tingling, L. Li, Z. Yuan, *J. Rare Earth.,* 2012, **30**, 753-756. (d) L. Fang, Y. Yao, Y. Zhang, Q. Shen, Y. Wang, *Z. Anorg. Allg. Chem.*, 2013, **639**, 2324-2330.
9. (a) C. X. Lam, S. H. Teoh, D. W. Hutmacher, *Polym. Int.,* 2007, 718. (b) M. J. Jenkins, K. L. Harrison, M. M. C. G. Silva, M. J. Whitaker, K. M. Shakesheff, S. M. Howdle, *Eur. Polym. J.,* 2006, **42**, 3145. (c) D. W. Hutmacher, T. Schanz, I. Zein, K. W. Ng, S. Hin, T. Kim, C. Tan, *J. Biomed. Mater. Res.*, 2001, **55**, 203.
10. Y. Ikada, H. Tsuji, *Macromol. Rapid. Commun.,* 2000, **21**, 117.
11. J. L. Hedrick, T. Magbitang, E. F. Connor, T. Glauser, W. Volksen, C. J. Hawker, V. Y. Lee, R. D. Miller, *Chem. Eur. J.,* 2002, **8**, 3308.
12. P. Joshi, G. Madras, *Polym. Degrad. Stab.,* 2008, **93**, 1901.
13. (a) M. Wedler, H. W. Roesky, F. T. Edelmann, *J. Organomet. Chem.*, 1988, **345**, C1. (b) M. Wedler, M. Noltemeyer, F. T. Edelmann, *Angew. Chem. Int. Ed. Engl.,* 1992, **31**, 72. (c) M. Wedler, F. Knösel, M. Noltemeyer, F. T. Edelmann, *J. Organomet. Chem.*, 1990, **388**, 21. (d) M. Müller, V. C. Williams, L. H. Doerrer, M. A. Leech, S. A. Mason, M. L. H. Green, K. Prout, *Inorg. Chem.*, 1998, **37**, 1315. (e) P. B. Hitchcock, M. F. Lappert, D.-S. Liu, *J. Organomet. Chem.*, 1995, **488**, 241. (f) W. J. Evans, J. R. Walensky, J. W. Ziller, A. L. Rheingold, *Organometallics*, 2009, **28**, 3350. (g) W. J. Evans, J. R. Walensky, J. W. Ziller, *Chem. Eur. J*., 2009, 12204. (h) W. J. Evans, J. R. Walensky, J. W. Ziller, *Chem. Commun*., 2009, 7342. (i) W. J: Evans, J. R. Walensky, J. W. Ziller, *Inorg. Chem*., 2010, **49**, 1743. (j) W. J. Evans, J. R. Walensky, J. W. Ziller, *Organometallics*, 2010, **29**, 101. (k) C. V. Villiers, P. Thuéry, M. Ephritikhine, *Eur. J. Inorg. Chem*., 2004, 4624. (l) E. Rabinovich, S. Aharonovich, M. Botoshansky, M. S. Eisen, *Dalton Trans*., 2010, **39**, 6667. (m) E. Domeshek, R. J. Batrice, S. Aharonovich, B. Tumanskii, M. Botoshansky, M. S. Eisen, *Dalton Trans*., 2013, **42**, 9069.
14. G. Hafelinger, K. H. Kuske, In *The Chemistry of the amidines and imidates*, Eds. S. Patai, Z. Rappoport, Wiley Chichester, Volume 2, 1991, pp. 1-100.
15. (a)http://www.ccdc.cam.ac.uk/Solutions/CSDSystem/Pages/CSD.aspx (b) W. J. Evans, J. R. Walensky, J. W. Ziller, A. L. Rheingold, *Organometallics*, 2009, **28**, 3350. (c) W. Ren, G. Zi, D.-C. Fang, M. D. Walter, *J. Am. Chem. Soc*., 2011, **133**, 13183. (d) M. Guymont, J. Livage, C. Mazières, *Bull. Soc. Fr. Mineral. Cristallogr.*, 1973, **96**, 161.
16. P. C. Burns, R. C. Ewing, F. C. Hawthorne, *Can. Mineral*., 1997, **35**, 1551.
17. X. Wang, L. Andrews, *Phys. Chem. Chem. Phys*., 2005, **7**, 3834.
18. A. L. Ward, H. L. Buckley, W. W. Lukens, J. Arnold, *J. Am. Chem. Soc*., 2013, **135**, 13965.
19. (a) S. E. Denmark, G. L. Beutner, T. Wynn, M. D. Eastgate, J. Am. Chem. Soc., 2005, 127, 3774. (b) A. R. Bassindale, P. G. Taylor Reaction Mechanisms of Nucleophilic Attack at Silicon, *in Organic Silicon Compounds Volume 1 and Volume 2,* 1989 S. Patai, Z. Rappoport, Eds., John Wiley & Sons, Ltd, Chichester, UK. (c) M. Cypryk, Y. Apeloig, *Organometallics*, 2002, **21**, 2165. (d) T. Segmüller, P. A. Schlütter, M. Drees, A. Schier, T. Straßner H. H. Karsch, *J. Organomet. Chem*., 2007, **692**, 2789. (e) T. Segmüller, PhD Thesis, Technische Universität München, 2003.
20. (a) T. Andrea, E. Barnea, M. S. Eisen, *J. Am. Chem. Soc*., 2008, **130**, 2454. (b) S. D. Wobster, T. J. Marks, *Organometallics*, 2013, **32**, 2517. (c) E. Barnea, D. Moradove, J.-C. Berthet, M. Ephritikhine, M. S. Eisen, *Organometallics*, 2006, **25**, 320. (d) A. Walshe, J. Fang, L. Maron, R. J. Baker, *Inorg. Chem*., 2013, **53**, 9077. (e) C. E. Hayes, Y. Sarazin, M. J. Katz, J.-F. Carpentier, D. B. Leznoff, *Organometallics*, 2013, **32**, 1183. (f) W. Ren, N. Zhao, L. Chen, G. Zi, *Inorg. Chem. Commun*., 2013, **30**, 26. (g) I. S. R. Karmel, M. Botoshansky, M. Tamm, M. S. Eisen, *Inorg. Chem*., 2014, **53**, 694.
21. S. D. Bai, R.-Q. Liu, T. Wang, F. Guan, Y.-B. Wu, J.-B. Chao, H.-B. Tong, D.-S. Liu, *Polyhedron*, 2013, **65**, 161.
22. (a) I. A. Khan, H. S. Ahuja, *Inorg. Synth.*, 1982, **21**, 187. (b) T. Andrea, PhD Thesis, Technion, 2007.
23. T. Andrea, E. Barnea, M. Botoshansky, M. Kapon, E. Genizi, Z. Goldschmidt, M. S. Eisen, *J. Organomet. Chem*., 2007, **692**, 1074.
24. Kappa CCD Server Software; Nonius BV, Delft, The Netherlands, 1997.
25. Z. Otwinowski, W. Minor, *Methods Enymol*., 1997, **276**, 307.
26. G. M. Sheldrick, *Acta Crystallogr., Sect. A*., 1990, **A46**, 467.
27. ORTEP, TEXSAN Structure Analysis Package; Molecular Structure Corp., The Woodlands, TX, 1999.
28. Mercury Software from CCDC: http://www.ccdc.cam.ac.uk/Solutions/CSDSystem/Pages/Mercury.aspx.

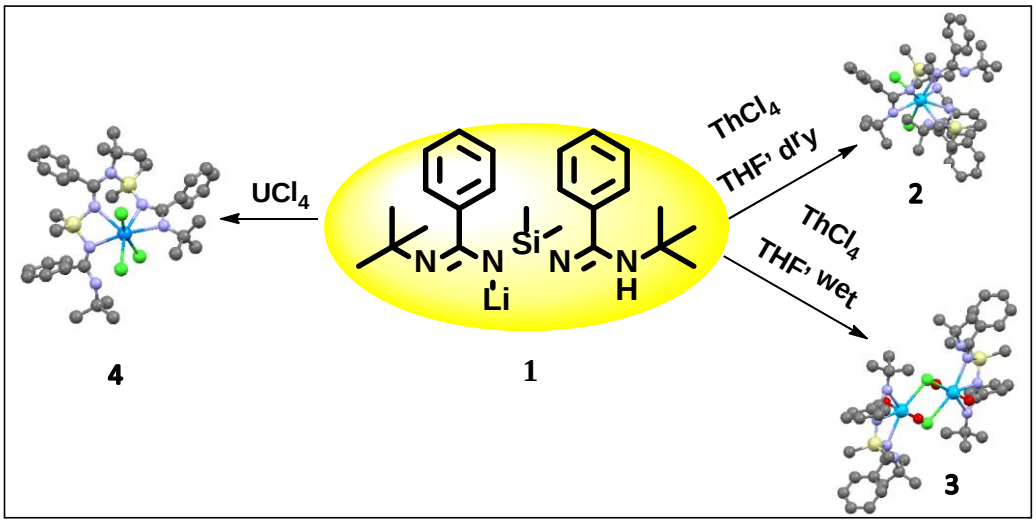


Ligand **1** reacts with $ThCl_4$ and $UCl_4$ yielding complexes **2** and **4**, respectively. Complex **3** is obtained from complex **2** displaying extremely short Th-OH bond distances.